Research Square

Preprints are preliminary reports that have not undergone peer review.
They should not be considered conclusive, used to inform clinical practice,
or referenced by the media as validated information.

Beyond keratinases: Oxidoreductase-Mediated Pathways Underlying Feather Degradation Mechanism by Streptomyces sp. G11C

Valentina González
Universidad Técnica Federico Santa María
Néstor Serna-Cardona
Universidad Técnica Federico Santa María
María José Vargas-Straube
Centro Regional de Estudios en Alimentos Saludables
Agustina Undabarrena
Universidad Técnica Federico Santa María
Roger Karlsson
University of Gothenburg
Leonarda Alarcon
University of Gothenburg
Michael Seeger
Universidad Técnica Santa María, Chile
Beatriz Cámara
beatriz.camara@usm.cl

Universidad Técnica Federico Santa María

Research Article

Keywords: marine Streptomyces, keratinolytic bacteria, keratinases, keratin degradation mechanism, proteomic analysis, feather degradation, disulfide reductase, oxidoreductases

Posted Date: September 2nd, 2026

DOI: https://doi.org/10.21203/rs.3.rs-10703291/v1

License: This work is licensed under a Creative Commons Attribution 4.0 International License.
Read Full License

Additional Declarations: No competing interests reported.

Beyond keratinases: Oxidoreductase-Mediated Pathways Underlying Feather Degradation Mechanism by *Streptomyces* sp. G11C

*Valentina González[1,2,3], Néstor Serna-Cardona[1,2,3], María José Vargas-Straube[5], Agustina Undabarrena[2], Roger Karlsson[6], Leonarda Alarcon[6], Michael Seeger[3,4] and Beatriz Cámara[2,3]**

[1]Departamento de Química y Medio Ambiente, Sede Viña del Mar, Universidad Técnica Federico Santa María, Viña del Mar 2520000, Chile;

[2]ActinoLab USM, Centro de Biotecnología "Daniel Alkalay Lowitt", Universidad Técnica Federico Santa María, Valparaíso 2390136, Chile;

[3]Millennium Nucleus Bioproducts, Genomics and Environmental Microbiology (BioGEM), Universidad Técnica Federico Santa María, Valparaíso 2390123, Chile;

[4]Laboratorio de Microbiología Molecular y Biotecnología Ambiental, Departamento de Química, Universidad Técnica Federico Santa María, Valparaíso 2390123, Chile;

[5]Centro Regional de Estudios en Alimentos Saludables, Valparaíso 2373223, Chile.

[6]Department of infectious diseases, Institute of Biomedicine, Sahlgrenska Academy, University of Gothenburg, Gothenburg 40530, Sweden.

*Corresponding author, e-mail: beatriz.camara@usm.cl

Abstract

Background. Feather waste is an abundant keratin-rich byproduct generated by the poultry industry that represents an important environmental challenge due to the recalcitrant nature of keratin. Although keratinolytic microorganisms have emerged as promising biotechnological tools for feather valorization, the molecular mechanisms underlying bacterial keratin degradation remain poorly understood. In this study, we investigated the protein machinery involved in keratin degradation by *Streptomyces* sp. G11C using a global label-free shotgun proteomic approach.

Results. Proteomic analysis of cellular and extracellular fractions collected after 3 and 5 days of cultivation identified 794 proteins, with proteases and oxidoreductases among the most abundant functional groups. An S8 serine protease and an M6 metalloprotease were identified as the major candidate keratinases, and their roles were experimentally validated through overexpression in *Streptomyces* sp. G11C, resulting in approximately 2.5-fold higher keratinolytic activity than the wild-type strain. Additional components, including lytic polysaccharide monooxygenases and dihydrolipoyl dehydrogenases, highlight oxidoreductase-mediated mechanisms for keratin denaturation and disulfide bond reduction, suggesting a previously unrecognized contribution to bacterial keratin degradation. Sulfite production was detected during feather degradation, although its relatively low concentration supports a predominant role for enzymatic disulfide reduction. In addition, proteins involved in sulfur metabolism, oxidative stress response, protein folding, and cellular adaptation, including γ-glutamyl transferase, catalases, DnaK, and TerD proteins, were identified, indicating coordinated physiological responses during keratin utilization.

Conclusions. Our findings support a multistep model of bacterial keratin degradation in which oxidoreductase-mediated destabilization of the keratin structure precedes extracellular proteolysis and is accompanied by metabolic and stress-adaptation processes. This work provides new

mechanistic insights into microbial keratin degradation, identifies novel enzymes potentially involved in this process, and expands the current understanding of bacterial keratin utilization, offering new opportunities for the development of sustainable biotechnological processes for feather waste valorization.

Keywords. marine *Streptomyces*, keratinolytic bacteria, keratinases, keratin degradation mechanism, proteomic analysis, feather degradation, disulfide reductase, oxidoreductases.

Background

Poultry meat is among the most widely consumed animal-derived foods worldwide, with demand projected to increase by 21% by 2034 [1]. This sustained growth has intensified poultry production and the generation of agro-industrial residues. Among these, feathers constitute one of the most abundant and recalcitrant by-products, with an estimated annual production of 8.5 million tons worldwide [2]. Traditionally, a large portion of these wastes have been either discarded or incinerated, leading to significant environmental concerns [3]. However, feathers contain up to 90% keratin, making them a valuable source of amino acids for animal feed, fertilizers, and emerging biomedical applications [4–6]. Despite their biotechnological potential, the structural recalcitrance of keratin requires harsh processing conditions that hinder its large-scale valorization [7]. Current physicochemical treatments used to produce feather meal are energy-intensive, reduce nutritional quality, and release polluting gases such as sulfur compounds and ammonia [8]. Therefore, sustainable strategies for feather waste valorization are urgently needed to mitigate environmental impacts and contribute to the transition toward a circular economy.

Keratinolytic microorganisms and their enzymes have emerged as a promising alternative for feather waste management. Among these, bacteria such as *Bacillus* and *Streptomyces* are

recognized as major producers of keratinases, a subset of proteases capable of hydrolyzing keratin-rich substrates [9,10]. However, studies have shown that purified keratinases alone are insufficient for efficient keratin hydrolysis [11]. The highly recalcitrant structure of keratin, composed of tightly packed polypeptide chains stabilized by disulfide bonds, hydrogen bonds, hydrophobic interactions, and post-translational modifications, requires the coordinated action of proteolytic and reducing systems for effective degradation [12]. Disulfide bond disruption can occur through multiple pathways, including sulfite-mediated thiolysis [13–15], enzymatic reduction by disulfide reductases [16], cell-associated redox processes at the membrane level [17], and mechanical pressure mediated by the mycelial growth of filamentous microorganisms [11,15,18]. Despite these advances, the mechanisms underlying keratin degradation in most microorganisms remain poorly understood, largely due to the historical emphasis on keratinases whereas other complementary biological processes have received comparatively less attention [11,19]. Further research is required to elucidate the key enzymes governing this complex degradation system.

In this study, we investigated the molecular basis of feather keratin degradation by *Streptomyces* sp. G11C, a marine bacterium previously shown to exhibit strong keratinolytic activity [20]. While earlier work identified key keratinolytic proteases through zymography-guided proteomic approaches, the broader molecular processes underlying keratin degradation remain poorly understood. To address this knowledge gap, we performed a comprehensive, non-targeted proteomic analysis of feather-based cultures, enabling system-level characterization of proteins associated with keratin breakdown. Beyond peptide hydrolysis, the identified proteins suggest coordinated roles in disulfide and glycosidic bond cleavage, as well as filamentous growth, substrate colonization, and cellular adaptation. Notably, several of these components have been rarely described in other keratinolytic bacteria, suggesting previously underappreciated

mechanisms involved in keratin degradation. By moving beyond a keratinase-centric perspective, this work expands the mechanistic understanding of keratin biodegradation and supports the development of more efficient and sustainable strategies for feather waste valorization, including strain engineering and enzyme-based biotechnological applications.

Methods

Bacteria and Growth Conditions

Streptomyces sp. G11C, previously selected for its high keratinolytic potential [20], was cultured in a medium (pH 7.2) with the following composition per liter: 15 g of whole turkey feathers, 2 g of NaCl, 0.51 g of $MgSO_4*7H_2O$, 1 g of KH_2PO_4, 1.5 g of K_2HPO_4, and 10 mL of a trace element solution as previously described [20]. Turkey feathers, obtained from a local poultry slaughterhouse, were washed several times with tap water, 70% v/v ethanol, and distilled water, followed by drying at 60°C for 24 h. Cultures were carried out in 250 mL Erlenmeyer flasks containing 50 mL of culture medium, at 200 rpm and 30°C. For the proteomic analysis and reductase activity, cultures were grown for 3 and 5 days. Each experiment was conducted in triplicate.

Determination of keratinolytic activity, amino groups, sulfhydryl groups and protein content

Keratinolytic activity was determined using keratin azure (Sigma-Aldrich, St. Louis, MO, USA) as previously described [20]. Briefly, 200 µL of culture supernatant was incubated with 800 µL of 0.4% (w/v) keratin azure in 50 mM potassium phosphate buffer (pH 8.0) at 37 °C and 350 rpm for 1 h. After centrifugation (13,000 rpm, 10 min), the absorbance of the released azo dye was measured at 595 nm. A control sample included buffer and substrate without the enzyme. One unit

of keratinolytic activity was defined as the enzyme quantity needed to increase absorbance by 0.01 units in an hour under these conditions. Concentration of α-amino groups was determined following the OPA method described by Nielsen *et al*. [21]. For sample measurement, 200 µL of culture supernatant was mixed with 1.5 mL of OPA reagent containing DTT. After two min of reaction, absorbance was measured at 340 nm and α-amino group concentration was calculated using a serine standard curve. Free sulfhydryl groups (-SH) were quantified using the DTNB assay (5,5′-dithio-bis-(2-nitrobenzoic acid)) as previously described [22]. Briefly, 200 µL of culture supernatant was mixed with 1.7 mL of 20 mM potassium phosphate buffer (pH 6.6) and 100 µL of 10 mM DTNB in methanol. After 5 min of reaction, absorbance was measured at 412 nm and sulfhydryl group concentrations were calculated using a cysteine standard curve. Protein concentration was determined by the Bradford method [23], following the manufacturer's instructions for the Bio-Rad assay reagent (Bio-Rad, Hercules, CA, USA), with BSA used as standard.

Evaluation of disulfide reductase activity

To determine whether reductase activity is associated with cells or secreted components, a disulfide bond reduction assay was performed using different fractions of the *Streptomyces* sp. G11C culture. Strain G11C was cultured on feathers as the sole carbon and nitrogen source for 3 and 5 days. Cultures were then centrifuged to separate the supernatant and cell pellet. Pellets were washed twice with sterile 0.85% NaCl, and a portion of the washed cells was lysed using lysozyme (10 mg/mL) and proteinase K (20 mg/mL) in PBS buffer (pH 7.2) at 37 °C for 45 min. Lysed sample was centrifuged for 2 min at 13,000 rpm to collect intracellular components that were brought to a final volume of 2 mL with PBS buffer. Finally, 2 mL of each fraction: supernatant

(extracellular fraction), cells (whole-cell fraction, including membrane-associated redox properties and intracellular components), and cell lysate (intracellular contents released after cell disruption), were incubated with 3 mL of PBS containing either 2 mM oxidized glutathione (GSSG) or 2 mg/mL ground feathers as disulfide-containing substrates. Samples were incubated overnight at 30 °C and 200 rpm. Sulfhydryl group concentration was determined using DTNB as previously described. Measurements were performed after 30 min and 18 h of incubation to evaluate cumulative substrate modification, considering the limited accessibility of the keratin substrate. Controls consisted of substrate incubated with uninoculated culture medium.

Extracellular protein extraction

Culture broths collected after 3 and 5 days of incubation were centrifuged (13,000 rpm, 15 min) to separate the cell pellet and supernatant. Cell pellet was reserved for protein extraction as described in the following section. The supernatant was filtered (0.2 µm), and extracellular proteins were recovered by trichloroacetic acid (TCA) precipitation as described by Huang *et al*. [24], with minor modifications. Proteins were precipitated by mixing 18 mL of the filtered supernatant with 2 mL of 100% TCA (final concentration 10% v/v) and stored at -20°C overnight. Subsequently, samples were thawed and centrifuged at 13,000 rpm for 30 min at 4°C. Protein pellet was washed three times with 1 mL of cold acetone and then centrifuged at 13,000 rpm for 5 min at 4°C. Finally, the pellet was air-dried in a fume hood. Prior to analysis by mass spectrometry, the proteins were reconstituted using digestion buffer (6M Urea, in 50 mM Tris-HCl, pH 8).

Bacterial cell lysate protein extraction

Cell pellet samples recovered after 3 and 5 days of culture were washed twice with sterile PBS buffer (pH 7.4), followed by centrifugation at 5000 rpm for 5 min. Pellet obtained was resuspended in 500 µL of 50 mM EDTA buffer (pH 8) and incubated with 50 µL of lysozyme (20 mg/mL) at 37 °C and 300 rpm for 30 min. Then, samples were centrifugated at 13,000 rpm for 2 min, and pellet was resuspended in 1.5 mL of lysis buffer (7M urea, 2M thiourea, and 2% w/v CHAPS). Samples were subjected to a freeze–thaw cycle (-20 °C for 30 min followed by 32 °C for 30 min), and proteins were recovered from the supernatant after centrifugation at 7000 rpm for 2 min.

Sample preparation for mass spectrometry

Proteins from extracellular and cellular fractions were reconstituted and diluted to ≤1 mg/mL in digestion buffer (6 M urea, 50 mM Tris-HCl, pH 8), reduced with 10 mM DTT for 1 h at room temperature, and alkylated with 30 mM iodoacetamide for 1 h in the dark. Proteins were then digested overnight at 37 °C with trypsin (Pierce MS Grade, Thermo Fisher Scientific) at a 1:50 (w/w) enzyme-to-protein ratio. Digestion was stopped by adding formic acid to a final concentration of 5% (v/v), and peptide-containing supernatants were recovered by centrifugation (13,000 rpm, 10 min) and stored at −20 °C until mass spectrometry analysis.

Proteomic analysis and protein identification

Samples were purified using HiPPR detergent removal kit and Pierce peptide desalting spin columns (both Thermo Fisher Scientific), according to the manufacturer´s instructions, dried and reconstituted in 15 µL of 3% acetonitrile and 0.1% trifluoroacetic acid. LC-MS analysis was performed on an Orbitrap Exploris mass spectrometer interfaced with an Easy-nLC1200 liquid chromatography system (both Thermo Fisher Scientific). Peptides were trapped on an Acclaim

Pepmap 100 C18 trap column (100 µm x 2 cm, particle size 5 µm, Thermo Fisher Scientific) and separated on an in-house packed analytical column (35 cm x 75 µm, particle size 3 µm, Reprosil-Pur C18, Dr. Maisch) at a flow of 300 nL/min using a gradient from 4% to 80% acetonitrile in 0.2% formic acid over 90 min. Of 15 µL sample, 2 µL were injected for analyses. The instrument operated in data-dependent mode where the precursor ion mass spectra were acquired at a resolution of 120,000, m/z range 380-1500. The most intense ions with charge states 2 to 6 were selected for fragmentation using HCD at collision energy settings of 30 and dynamic exclusion 30 s, 10 ppm. The isolation window was set to 0.7 Da and MS2 spectra were recorded at a resolution of 30,000.

Raw files were searched for identification using Proteome Discoverer version 2.4 (Thermo Fisher Scientific). Data were matched against sequences from the *Streptomyces* sp. G11C genome (NCBI RefSeq assembly: GCF_018638335.1)[25] using Sequest as a search engine. The precursor mass tolerance was set to 7 ppm and fragment mass tolerance to 0.3 Da. Tryptic peptides were accepted with one missed cleavage and Percolator in combination with Protein FDR Confidence at least medium (5%FDR) was selected. Protein abundance was estimated using peptide-spectrum matches (PSMs), a semi-quantitative indicator of relative protein abundance [26]. Because spectral counts are influenced by protein length and peptide detectability, PSMs were used primarily to identify proteins enriched across fractions and time points, rather than to infer absolute stoichiometries. Results from two biological replicates were considered, and proteins supported by at least one unique peptide in at least one replicate (≥1 high-quality PSM) were retained [27]. Raw proteomic data are provided in Table S1.

Bioinformatic analysis of the detected proteins

Subcellular localization and signal peptides of the detected proteins were predicted using CELLO v2.5 [28] and SignalP 5.0 [29], respectively. Functional annotation and assignment to clusters of orthologous groups (COGs) were performed using eggNOG 5.0 server [30] and verified by manual curation with the NCBI BLAST server (https://blast.ncbi.nlm.nih.gov/Blast.cgi). Protein abundance, estimated from PSM values, was visualized as a heatmap using TBtools [31].

Phylogenetic analysis of TerD-type proteins

TerD proteins identified in strain G11C were included in a phylogenetic analysis and compared with homologs from *Streptomyces coelicolor* A3(2) (Table S2). Selected amino acid sequences were aligned using MAFFT v7.511 [32]. Alignments were manually trimmed using AliView v1.28 [33]. Phylogenetic reconstruction was performed using Bayesian Markov Chain Monte Carlo (MCMC) inference in MrBayes v3.2.7 [34]. Two independent runs were conducted with a mixed amino acid substitution model, each consisting of 500,000 generations (two chains per run, sampling every 1,000 generations). The consensus tree was built following a burn-in process, discarding 25% of the trees. Posterior probabilities were used to support internal branches. Editing and visualization of the phylogenetic tree were carried out using iTOL v5 [35].

Detection of sulphite in feather culture of *Streptomyces* sp. G11C

Sulphite production was evaluated in culture supernatants collected after 3 and 5 days of culture by $BaCl_2$ precipitation and $KMnO_4$ decolorization assays [36]. A 0.1 M sodium sulphite solution and distilled water were used as positive and negative controls, respectively. Sulphite was further confirmed and quantified using the Monier–Williams method, based on SO_2 release after acidification and subsequent capture and titration [37].

Structural studies by scanning electron microscopy

To characterize feather degradation and bacterial colonization, cultures were incubated for 24, 72, and 120 h at 30 °C and 200 rpm in the previously described medium. Culture samples with digested feathers were filtered using Whatman grade 3 filter paper. Samples were then trimmed into 1cm^2 pieces, lyophilized and gold-coated with a SPI Sputter coater (USA). Scanning Electron Microscopy (SEM) images were recorded using an EVO MA 10 Carl Zeiss microscope (Germany) at an accelerating voltage between 10 and 15 kV. Samples were examined at 24X–29X magnification to evaluate overall feather degradation and at 800X–10,000X magnification to assess feather structure, mycelium formation, and spore production.

Overexpression of keratinase candidate genes

To evaluate the role of selected proteases in feather degradation, the genes *kerS8* and *kerM6*, identified among the most abundant proteases in the proteomic analysis, were overexpressed in *Streptomyces* sp. G11C. Overexpression plasmids (pSET-kerS8 and pSET-kerM6) were generated by cloning each gene into the XbaI/EcoRI sites of the integrative vector pSET152Ec under the control of the constitutive ermE promoter *Streptomyces* spp. [38]. Constructs were introduced into strain G11C by intergeneric conjugation from *Escherichia coli* ET12567/pUZ8002 as previously described [39], and successful integration was confirmed by PCR and sequencing. To evaluate the effect of gene overexpression on keratin degradation, wild-type G11C and the overexpression strains G11C-kerS8 and G11C-kerM6 were cultured in triplicate on chicken feathers using the saline medium described above. Cultures were adjusted to an initial OD600 of 0.2, and samples

were collected after 3 and 5 days. Keratinolytic activity, free amino groups, sulfhydryl groups, and soluble protein were quantified as described above.

Statistical analysis

All experiments were conducted using three independent cultures, and results were expressed as mean ± standard deviation. Statistical analyses were conducted by one-way ANOVA followed by Tukey–Kramer multiple comparisons test using GraphPad Prism 7 software [40]. Differences were considered significant if the p-value was less than 0.05.

Results and discussion

Physiological and Proteomic Overview of Feather Degradation by *Streptomyces* sp. G11C

Streptomyces sp. G11C was previously shown to exhibit strong keratinolytic activity achieving approximately 80% feather solubilization within five days of culture [20]. Although key keratinolytic proteases produced by this strain have been identified through zymography-guided proteomic analyses [20], the broader molecular mechanisms underlying keratin degradation remain largely unexplored. To address this gap, we performed a global label-free shotgun proteomic analysis of feather-based cultures to obtain a system-level view of the process, encompassing not only proteolysis but also complementary mechanisms such as disulfide bond reduction, keratin structural modification, and developmental processes associated with substrate colonization.

During a 7-day culture of strain G11C on feather keratin, the concentrations of sulfhydryl and free amino groups displayed distinct kinetic profiles, indicative of disulfide bond reduction and peptide bond hydrolysis, respectively (Figure 1a). Sulfhydryl group concentrations increased

progressively, reaching approximately 300 µM around day 4 before stabilizing, suggesting that reductive processes are more pronounced during the early stages of growth. In contrast, amino group concentrations increased continuously throughout culture, consistent with sustained keratinolytic activity, ultimately leading to the complete degradation of feather structure (Figure 1b). Based on these profiles, days 3 and 5 were selected for proteomic analysis as representative stages of early keratin destabilization and advanced proteolytic degradation, respectively. In addition, to distinguish proteins directly secreted into the extracellular environment from those associated with cellular metabolism and substrate colonization, cultures were further separated into extracellular (supernatant) and cellular fractions prior to proteomic analysis.

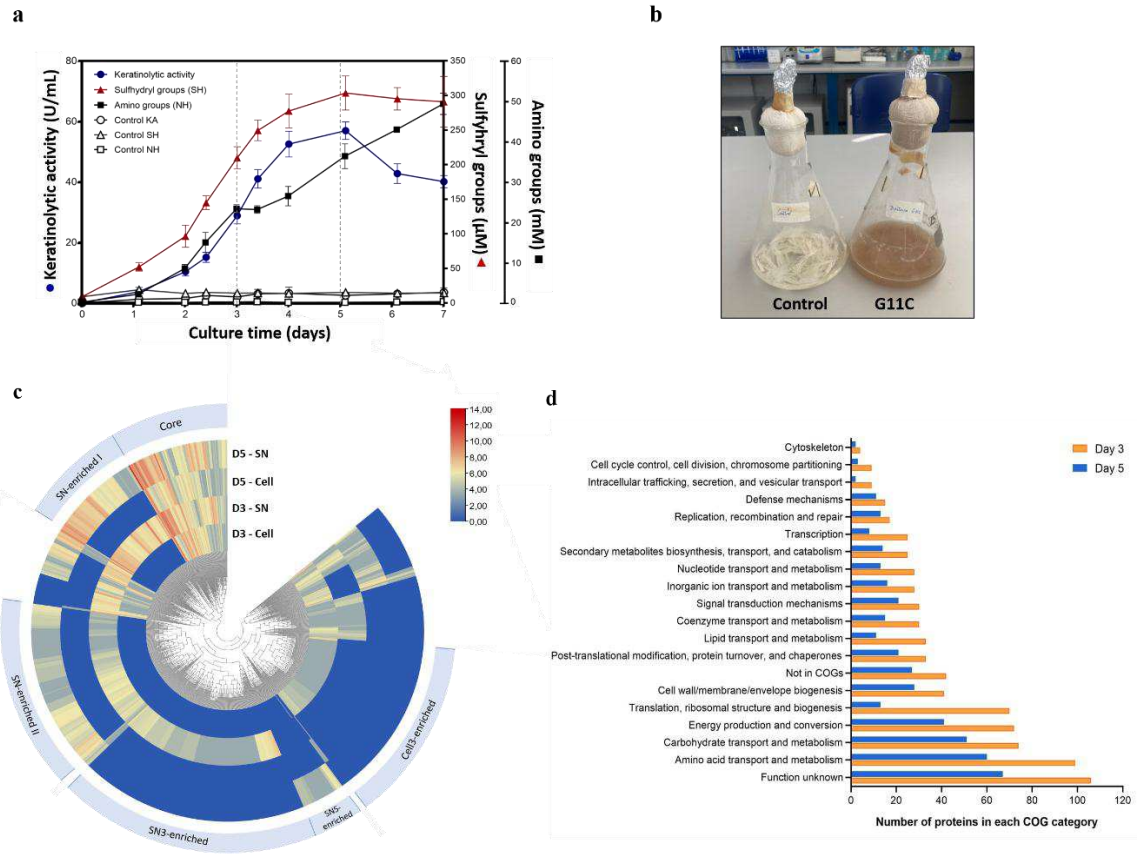


Figure 1. Feather degradation by *Streptomyces* sp. G11C and global proteomic analysis (a) Temporal changes in keratinolytic activity, sulfhydryl (SH) and amino (NH) group concentrations during a 7-day culture period. Dotted lines indicate sampling points selected for proteomic analysis. (b) Representative feather degradation in cultures

inoculated with strain G11C compared with an uninoculated control after 7 days of incubation. (c) Log-scale heatmap showing the abundance of 794 proteins identified in cellular (Cell) and culture supernatant (SN) fractions collected on days 3 and 5, expressed as peptide-spectrum matches (PSMs). Hierarchical clustering revealed protein groups enriched in cellular fractions (Cell3-enriched), supernatant fractions (SN-enriched I and II, SN3-enriched, and SN5-enriched), and a conserved core cluster. Numbers (3 and 5) indicate the culture day. (d) Functional classification of identified proteins according to Clusters of Orthologous Groups (COGs), comparing day 3 (orange) and day 5 (blue).

A total of 794 proteins were identified (Figure 1c, Table S1), representing approximately 13% of the predicted proteome [25]. Hierarchical clustering resolved proteins into a conserved core cluster and distinct groups preferentially enriched in cellular or extracellular fractions at different stages of feather degradation, revealing marked temporal and compartment-specific changes in protein abundance. Functional classification based on Clusters of Orthologous Groups (COGs) (Figure 1d) showed that proteins were broadly distributed across categories mainly associated with amino acid transport and metabolism (COG E; 12.2%), carbohydrate metabolism (COG G; 9.9%), and energy production and conversion (COG C; 9.6%), reflecting the metabolic adaptation required to sustain growth under feather-based culture conditions. Categories related to translation, ribosomal structure, and biogenesis (COG J; 8.6%) were particularly enriched at day 3, indicating elevated biosynthetic activity during the early stages of keratin degradation. In addition, functions linked to protein turnover and folding (COG O; 4.2%), membrane biogenesis (COG M; 5.2%), transcription (COG K; 3.1%), and signal transduction mechanisms (COG T; 3.8%) highlight the importance of protein quality control, cellular regulation, and stress adaptation during this process. Within this functional landscape, oxidoreductases (122 proteins) and proteases (61 proteins) were particularly abundant, suggesting a coordinated contribution of redox processes and proteolytic activity to keratin breakdown. Similar enrichment patterns have been reported in other

keratinolytic bacteria, including *Bacillus* [13] and *Fervidobacterium* [41], supporting the notion that keratin degradation relies on the integration of multiple biological processes beyond protease activity alone.

Temporal Proteome Dynamics During Feather Degradation

Temporal analysis revealed a pronounced shift in proteome composition between days 3 and 5, reflecting distinct physiological states during feather degradation (Figure 2a). Of the 794 proteins identified, 759 were detected on day 3 and 420 on day 5. While 385 proteins were shared between both time points, 374 were exclusively detected on day 3 and only 35 on day 5, indicating a substantially broader metabolic repertoire during the early stages of degradation.

Among the shared proteins, 77 proteins were classified within the conserved "Core" cluster identified in the hierarchical clustering analysis (Figure 1c). These proteins were detected in both cellular and supernatant fractions and include several of the most abundant components in the system, such as proteases, redox-associated enzymes (e.g., catalase, superoxide dismutase, thioredoxin-related proteins, and dihydrolipoyl dehydrogenase), molecular chaperones (e.g., DnaK), encapsulin nanocompartment proteins, and members of the TerD family (Figure 2b, Table S3). Among these, extracellular proteases, particularly S8 and S1 family peptidases, were most abundant in day 5 supernatant, consistent with sustained extracellular proteolysis during advanced stages of feather degradation. In contrast, many other proteins exhibited a more balanced distribution between cellular and extracellular fractions at both sampling times, suggesting broader physiological roles throughout the degradation process. Notably, several proteins typically considered intracellular, such as DnaK [42], encapsulin proteins [43], and TerD-family proteins [44], were also abundant in supernatant fractions. This observation may result from multiple

processes, including controlled cell lysis during the *Streptomyces* developmental cycle, in which programmed cell death and mycelial differentiation promote the release of intracellular proteins [45], as well as alternative export mechanisms such as extracellular vesicles and non-classical secretion pathways that have been increasingly recognized in *Streptomyces* [46,47]. Overall, this conserved set encompassed proteins involved in central metabolism, respiration, transport, redox balance, and stress response, supporting sustained energy production and cellular adaptation under keratin-degrading conditions across both early and late stages of the process.

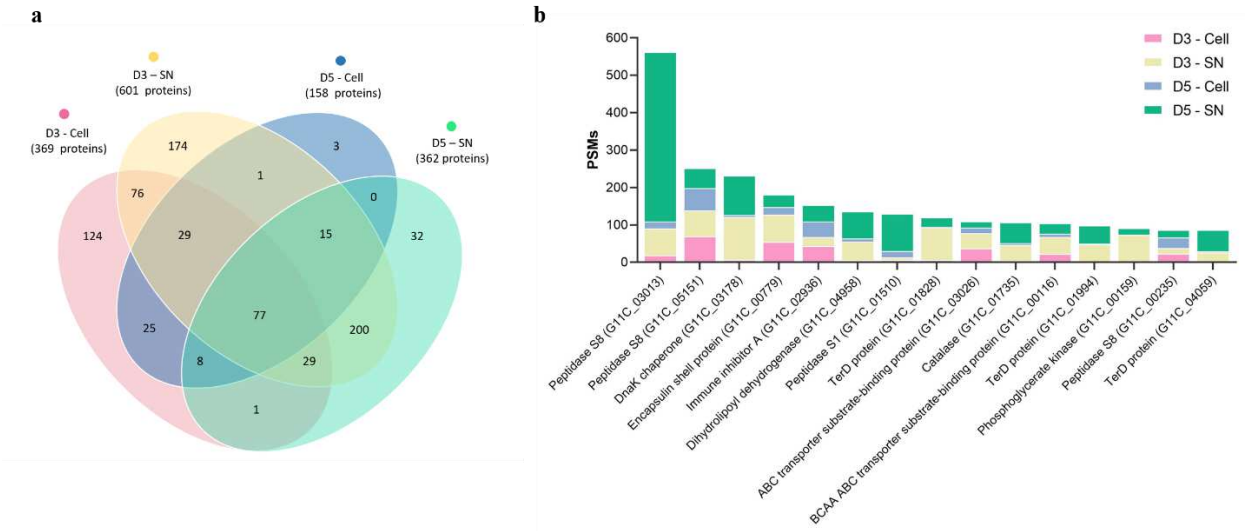


Figure 2. Temporal proteomic profiles of feather degradation by *Streptomyces* sp. G11C. (a) Venn diagram illustrating shared and unique proteins identified in cellular (Cell) and supernatant (SN) fractions at days 3 and 5 of culture. (b) Most abundant proteins detected in the proteome, showing their distribution between cellular and extracellular fractions and across sampling times. Protein abundance is expressed as PSMs.

Proteins enriched on day 3 (Cell3-enriched and SN3-enriched clusters) were primarily associated with active growth and feather depolymerization. These included proteins involved in translation, energy metabolism, extracellular proteolysis, and redox processes (e.g., ribosomal proteins, translation factors, proteases, oxidoreductases, and lytic polysaccharide

monooxygenases), consistent with elevated biosynthetic activity [48] and an intensive early-stage attack on the substrate. In contrast, proteins enriched at day 5 (SN5-enriched cluster) reflected a transition toward metabolic adaptation and stress response, including enzymes involved in alternative energy metabolism, redox homeostasis, carbohydrate utilization, and regulatory functions (e.g., succinate dehydrogenase, FAD- or NAD(P)-dependent oxidoreductases, β-N-acetylglucosaminidase, thioredoxin-disulfide reductase, and transcriptional regulators) [49–52]. This pattern suggests that, following extensive feather degradation, cellular activity transitions from substrate depolymerization to the assimilation of degradation products and maintenance of cellular homeostasis.

Overall, the proteomic profiles support a two-phase model of feather degradation by *Streptomyces* sp. G11C, consisting of an early degradative phase characterized by active proteolytic and redox processes, followed by a later stage focused on nutrient assimilation, metabolic optimization, and stress adaptation, while maintaining a conserved core of proteolytic and oxidative enzymes. The following sections examine the molecular mechanisms underlying these processes in greater detail.

Keratin denaturation and disulfide bond reduction mechanisms

Keratin consists of tightly packed α-helical or β-sheet filaments stabilized by extensive intermolecular disulfide bonds and post-translational modifications such as glycosylation, which limit enzymatic accessibility [12,53]. Consequently, efficient keratin degradation requires not only proteolysis but also complementary mechanisms that promote structural destabilization and disulfide bond reduction [11].

Reduction of disulfide bonds may be mediated by secreted components (e.g., sulfite or oxidoreductases), the redox potential of the cell membrane, or intracellular components (e.g., thioredoxin- and glutaredoxin-dependent systems) [11]. Reductase activity assays performed with feathers and oxidized glutathione (GSSG) as model disulfide-containing substrates, using supernatant, whole-cell, and cell-lysate fractions from *Streptomyces* sp. G11C cultures, revealed that the strongest disulfide bond-reducing activity was associated with the day 3 supernatant (Figures 3a and 3b). After 18 h of incubation, sulfhydryl group concentrations increased approximately fourfold with feathers and sevenfold with GSSG, whereas only a modest increase (~1.3-fold) was observed using the day 5 supernatant. These findings indicate that reducing capacity is highest during the early stages of feather degradation and is mainly associated with extracellular components, suggesting that disulfide bond reduction plays a more prominent role at the onset of keratin degradation.

Consistent with this observation, several proteins potentially involved in redox-mediated keratin destabilization were identified in the proteomic dataset. Among them, γ-glutamyl transferase (GGT; G11C_03747) was identified in the cellular fractions at both culture time points. This enzyme hydrolyzes glutathione (GSH), generating cysteinyl-glycine, a reducing dipeptide implicated in keratin degradation in recombinant *Escherichia coli* HB101 [54] and several keratinolytic *Bacillus* species [13,14,55,56]. Cysteinyl-glycine can be further hydrolyzed to cysteine, which may subsequently enter sulfur metabolic pathways leading to sulfite production [12,57], a well-established reducing agent capable of cleaving disulfide bonds through sulfitolysis [11,58]. Sulfite-mediated mechanisms have been reported in several keratinolytic microorganisms, including fungi and bacteria such as *Bacillus* [11,12,55,57,58] and *Streptomyces* [15]. Consistent with this mechanism, sulfite production by strain G11C was confirmed in culture supernatants

collected at days 3 and 5 using $BaCl_2$ precipitation, $KMnO_4$ decolorization, and the Monier–Williams assay (Figures 3c and 3d). Although genes encoding two cysteine dioxygenases and a putative sulfite exporter were identified in the genome, the corresponding proteins were not detected. Nevertheless, the presence of glutathione S-transferase (G11C_04119) supports active glutathione-related metabolism, which may be linked to sulfite production during keratin degradation. Together, these results indicate that sulfite participates in feather degradation by strain G11C, although the pathways responsible for its generation and export should be further investigated.

It is worth noting that, in actinomycetes, reducing equivalents may also derive from mycothiol (MSH), a glutathione analogue [59,60], previously associated with keratin degradation in *Streptomyces* sp. SCUT-3 [15]. Although genes involved in MSH biosynthesis are present in the G11C genome, the corresponding proteins were not detected in the proteomic dataset, suggesting that this system may be inactive under the tested conditions or expressed below the detection limit.

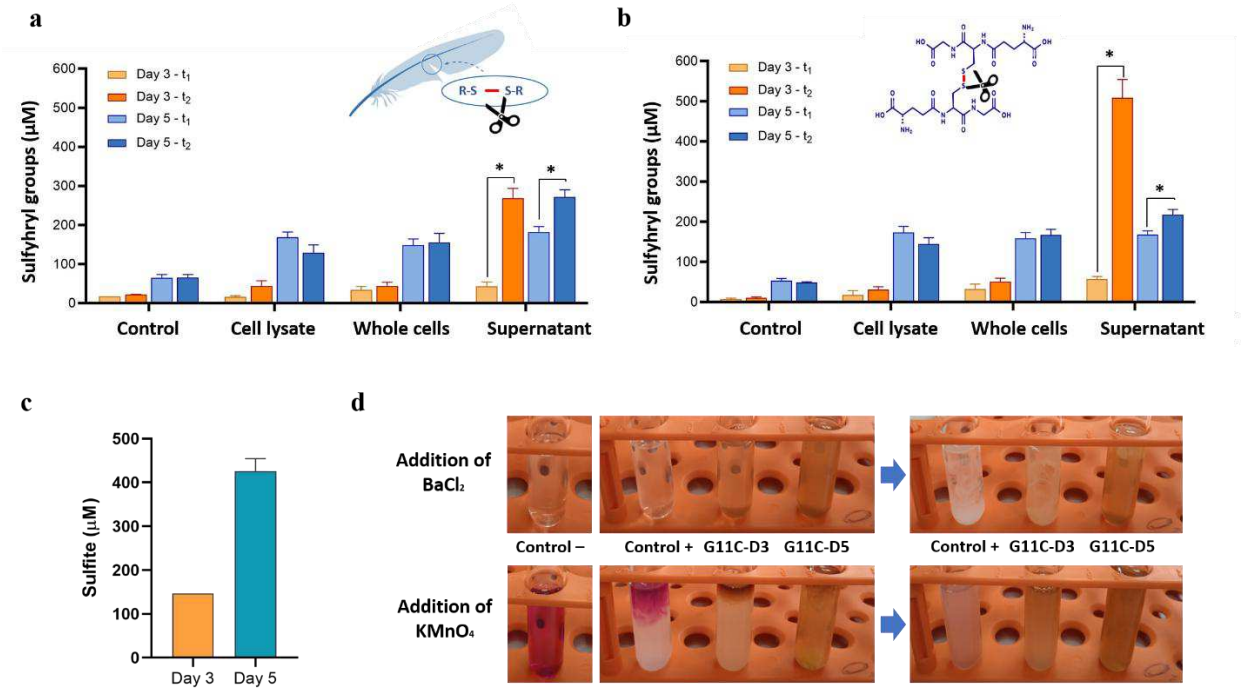


Figure 3. Disulfide bond-reducing activity and sulfite production during feather degradation by *Streptomyces* sp. G11C. (a) Changes in sulfhydryl (SH) group concentration using feathers as substrate and different culture fractions (cell lysate, whole cells, and supernatant) collected on days 3 and 5. (b) Reductase activity measured with oxidized glutathione (GSSG) as substrate using the same fractions. For panels (a) and (b), SH groups were quantified after 30 min (t_1) and 18 h (t_2) of incubation. Controls consisted of the corresponding substrate incubated with uninoculated culture medium. Data are presented as mean ± standard deviation; asterisks (*) indicate significant differences relative to t_1 ($p < 0.05$). (c) Sulfite concentration in culture supernatants collected on days 3 (G11C-D3) and 5 (G11C-D5), determined by the Monier–Williams method. (d) Qualitative detection of sulfite by $BaCl_2$ precipitation followed by $KMnO_4$ decolorization.

In addition to sulfite-mediated processes, enzymatic reduction of disulfide bonds has been proposed as a key mechanism contributing to keratin denaturation [11]. In keratinolytic bacteria such as *Bacillus* and *Stenotrophomonas*, disulfide reductases act synergistically with keratinases during feather and hair degradation [16,61–63]. One of the most abundant enzymes with potential disulfide-reducing activity in strain G11C cultures was dihydrolipoyl dehydrogenase (G11C_04958 and G11C_02220), detected at both time points. Although this flavin-dependent enzyme is best known as the E3 component of pyruvate and α-ketoglutarate dehydrogenase complexes [64], its catalytic mechanism has led to the proposal that it may also function as a disulfide reductase in keratin degradation [11]. However, to our knowledge, its involvement in keratin degradation has not yet been reported in keratinolytic microorganisms. Notably, dihydrolipoyl dehydrogenase was more abundant in extracellular fractions, where the strongest reductase activity was observed (Figures 1a and 1b). Furthermore, the relatively moderate sulfite concentrations detected in culture supernatants (~150 μM at day 3 and ~400 μM at day 5) suggest that sulfitolysis alone may not fully explain the observed extracellular reducing activity. Together, these observations identify dihydrolipoyl dehydrogenase as a strong candidate contributing to

disulfide bond reduction in strain G11C. Although direct biochemical validation is still required and will be essential to confirm this proposed role, this mechanism would differ from those previously proposed for *Streptomyces* spp., where disulfide bond reduction has been mainly attributed to sulfite production and cysteinyl-containing reducing molecules, as described for *Streptomyces* sp. SCUT-3 [15] or to redox processes dependent on metabolically active cells, as reported for *Streptomyces pactum* [17].

In addition to disulfide bond reduction, keratin accessibility may be influenced by post-translational modifications such as glycosylation, which contribute to the compact organization of keratin filaments and may hinder enzymatic attack [12]. In this context, four extracellular lytic polysaccharide monooxygenases (G11C_02990, G11C_02174, G11C_03647, and G11C_01517) were identified in the proteome of strain G11C, together with several glycosyl hydrolases (e.g., G11C_04355 and G11C_00680). LPMOs are copper-dependent oxidoreductases that catalyze the oxidative cleavage of recalcitrant polysaccharides such as cellulose, hemicellulose, and chitin [65,66].

These enzymes have previously been proposed to facilitate keratin degradation in filamentous fungi by targeting glycosylated regions of keratin filaments, thereby increasing substrate accessibility [12]. Given their extracellular localization, the LPMOs detected in G11C may perform a similar function. To our knowledge, neither LPMOs nor dihydrolipoyl dehydrogenase have previously been implicated in bacterial keratinolytic systems, suggesting potentially novel or underappreciated mechanisms contributing to keratin degradation by *Streptomyces* sp. G11C.

Extracellular keratinolytic proteases involved in keratin hydrolysis

Once keratin is destabilized, extracellular proteases can access the protein matrix and initiate hydrolysis [10]. A total of 61 proteases were identified in the proteome of strain G11C, including 20 proteins assigned to the conserved Core cluster (Figure 1c). This core repertoire comprises endopeptidases, mainly serine proteases (S8 and S1 families) and metalloproteases (M6, M7, M15, M23, and M41), together with exopeptidases (M17, M18, and M28 families) and oligopeptidases (S15 and S28 families) [67]. This combination suggests a coordinated system for progressive keratin breakdown into assimilable peptides and amino acids, consistent with reports highlighting the synergistic action of endo- and exoproteases in keratinolytic microorganisms [13,18,41,68,69].

Among the most abundant proteins detected were an S8 family serine protease (G11C_03013) and an M6 family metalloprotease (G11C_02936), both strong candidates for keratin degradation. The S8 protease was the most abundant protein identified (561 PSMs), consistent with our previous study that recognized it as a major contributor to the keratinolytic activity of strain G11C [20]. Its abundance increased markedly in the supernatant from day 3 to day 5 (72 vs 453 PSMs), supporting an important role during the later stages of feather degradation. Together with the sustained detection of other S8 and S1 proteases, these results reinforce the central role of subtilisin- and chymotrypsin-like enzymes in bacterial keratinolysis [10,70].

Additionally, a M6 metalloprotease, annotated as an immune inhibitor A, was also among the most abundant extracellular enzymes. Given its preference for hydrophobic C-terminal residues [71,72], it may be particularly suited for feather keratin degradation, a substrate enriched in hydrophobic amino acids [10]. Although M6 proteases have recently been implicated in keratin degradation in the fungus *Onygena corvina* [18], they remain largely unexplored in bacterial keratinolytic systems. Therefore, their identification in *Streptomyces* sp. G11C suggests a

potentially novel contribution of this protease class and expands the known diversity of enzymes involved in bacterial keratin degradation.

To validate the role of these proteases in keratin degradation, overexpression constructs were generated in the native strain *Streptomyces* sp. G11C using the integrative plasmid pSET152Ec, yielding the strains G11C-S8 and G11C-M6. At day 3, overexpression of both S8 and M6 proteases resulted in a significant increase in keratinolytic activity, reaching approximately 2.4–2.5-fold higher levels compared to the wild-type strain (WT), along with enhanced release of sulfhydryl and amino groups (Figure 4). Notably, M6 overexpression led to a more pronounced increase in amino group release at this early stage, suggesting a potentially efficient role in peptide generation during initial keratin breakdown. At later time points (day 5), the differences between the overexpression strains and the native strain became less pronounced, although keratinolytic activity remained elevated. Overall, these results support the involvement of both proteases as functional keratinases, contributing to the keratin degradation process, with potentially distinct roles at different stages of substrate utilization.

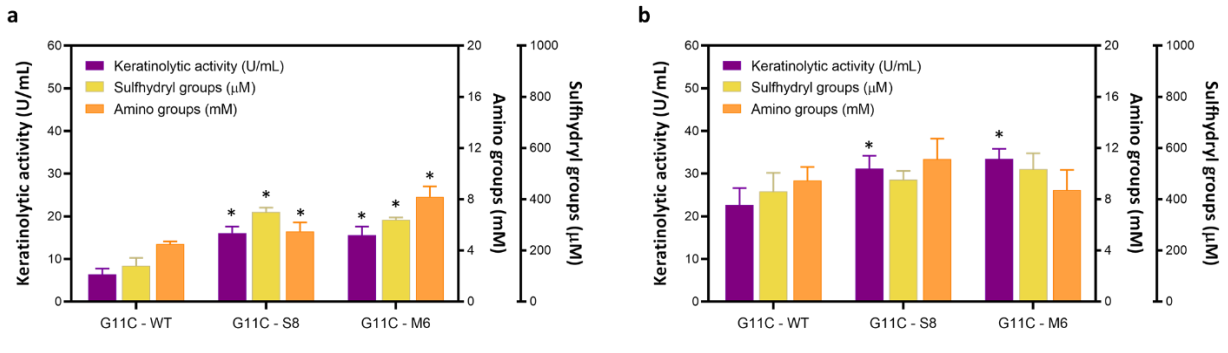


Figure 4. Functional validation of S8 and M6 proteases in keratin degradation by overexpression in *Streptomyces* sp. G11C. Keratinolytic activity, sulfhydryl group and amino group concentration were measured in cultures of the wild-type strain G11C-WT and overexpression strains G11C-S8 and G11C-M6 at days (a) 3 and (b) 5, respectively. Data are presented as mean ± SD. Asterisks (*) indicate statistically significant differences compared to the wild-type strain (WT) ($p < 0.05$).

Complementary pathways supporting keratin utilization: peptide assimilation, transport, and redox homeostasis

In addition to extracellular proteolysis, several intracellular and membrane-associated processes were detected that likely support the assimilation and metabolic utilization of keratin-derived products. Intracellular peptidases, including aminopeptidase N (G11C_05149) and leucyl aminopeptidase (G11C_00115), were detected at high abundance and are expected to complete peptide turnover by generating free amino acids from imported oligopeptides [67,73,74]. Consistent with this, multiple transport-related proteins were also detected: ABC transporter substrate-binding proteins (G11C_03026 and G11C_00116), which mediate ATP-dependent uptake of amino acids and peptides [75], and MFS transporters (G11C_05075 and G11C_03897), acting as complementary uptake systems driven by proton motive force [76]. Similar transport systems have been reported in other keratin-degrading microorganisms, including *Fervidobacterium* spp. [41], *Bacillus* sp. 8A6 [13], *Purpureocillium lilacinum* GZAC18-2JMP [69], and *Pseudomonas aeruginosa* Gxun-7 [77], highlighting their conserved role in nutrient assimilation from keratin-rich substrates. In parallel, enzymes associated with central metabolism and redox balance were detected, including the previously discussed dihydrolipoyl dehydrogenases (G11C_04958 and G11C_02220) and components of the succinate dehydrogenase complex (G11C_00420–G11C_00423), reflecting active electron transfer and energy generation during growth on keratin [64,78,79]. The presence of oxidative stress response enzymes, such as catalases (G11C_01735), superoxide dismutases (G11C_00771), and thioredoxin-related proteins (G11C_02846, G11C_02847, G11C_03466), further supports the existence of an active antioxidant defense system (Figure S1) [80–82]. This is consistent with

conditions expected during keratin degradation, where reactive oxygen species (ROS) formation may be intensified by elevated respiratory activity, oxidoreductase-mediated reactions, redox-active metal ions supplied by trace elements in the culture medium, and disulfide bond reduction processes associated with sulfur metabolism [77,80,81].

In addition, stress-associated proteins such as the molecular chaperone DnaK (G11C_03178), predominantly detected in extracellular fractions, may contribute to the stabilization or refolding of secreted enzymes [42,83–85], while the encapsulin nanocompartment protein (G11C_00779) suggests a potential role in the organization or protection of redox-related processes during early stages of keratin degradation [43,86]. Together, these findings indicate that keratin degradation in *Streptomyces* sp. G11C relies on coordinated mechanisms of nutrient assimilation, redox homeostasis, and stress adaptation that sustain cellular growth on this recalcitrant substrate.

Developmental and morphological processes associated with feather degradation

Beyond metabolic and hydrolytic enzymes, the proteome of *Streptomyces* sp. G11C revealed numerous proteins associated with cell envelope dynamics and morphological differentiation, suggesting that feather degradation is tightly coupled to developmental processes characteristic of filamentous actinobacteria. Among these, nine of the thirteen TerD-encoding genes present in the genome were detected during growth on feathers (Figure 5a), with three homologs (G11C_01828, G11C_01994, and G11C_04059) showing higher abundance on day 3 than on day 5. Phylogenetic analysis further revealed that the most abundant TerD proteins clustered with previously characterized Tdd homologs (Tdd8 and Tdd13) from *Streptomyces coelicolor,* which have been implicated in morphological development and stress adaptation [87,88]. In general, TerD proteins are thought to form part of membrane-associated metal-sensing complexes that couple metal

543 recognition with regulatory signaling and DNA-associated processes in bacterial stress response
544 systems [44]. In *Streptomyces*, they have been linked to morphological differentiation, stationary-
545 phase adaptation, programmed cell death, and stress responses, with specific homologs such as
546 Tdd8 associated with calcium homeostasis [45,87–90]. The elevated expression of these homologs
547 during the early stages of culture suggests that TerD-mediated pathways may contribute to the
548 physiological adaptation required for growth on feather keratin, potentially including responses to
549 the redox challenges associated with its degradation.

550 Consistent with active morphological remodeling, several enzymes involved in cell wall
551 dynamics were also detected, including peptidoglycan hydrolases, such as M23 and M15
552 metallopeptidases (G11C_00564, G11C_04917 and G11C_04461), lysozyme (G11C_02544), as
553 well as lytic polysaccharide monooxygenases (e.g., G11C_02990, G11C_02174), suggesting
554 ongoing cell wall turnover and structural plasticity during growth [67,91,92]. Such processes are
555 essential for hyphal extension [91,93], and may therefore facilitate mechanical interaction with the
556 keratin substrate, enhancing penetration and localized enzyme secretion. Comparable strategies
557 have been described in fungal systems, in which glycoside hydrolases from the GH16 and GH17
558 families contribute to cell wall plasticity during keratin degradation [18]. To our knowledge, the
559 contribution of cell wall remodeling processes to keratin degradation has not previously been
560 discussed in keratinolytic *Streptomyces*. The enzymes identified here suggest that morphological
561 plasticity and hyphal extension may represent an additional, previously underappreciated
562 component of feather degradation by filamentous bacteria.

563 Microscopic observations further supported a close association between feather degradation
564 and the developmental cycle of strain G11C. SEM images (Figure 5b and 5c) revealed that, during
565 the first 24 h, thin hyphae tightly adhered to the rachis and barbules, progressively expanding to

566 form a dense mycelial network covering the feather surface. By 72 h, a compact mycelial layer
567 was established, accompanied by the formation of pores and fissures that facilitated hyphal
568 penetration into the feather matrix and progressive structural disruption. At later stages (120 h),
569 abundant spores with characteristic ring-like morphology were observed, coinciding with
570 advanced substrate degradation and nutrient depletion.

571 These observations suggest that early hyphal adhesion likely promotes localized enzyme
572 secretion and initial keratin breakdown, while subsequent penetration enhances continued
573 substrate degradation. Similar substrate invasion mechanisms have been described in keratinolytic
574 fungi as part of mechanical keratinolysis, where hyphal growth physically disrupts the keratin
575 matrix prior to enzymatic hydrolysis [18,94]. Although the molecular basis of this process remains
576 unclear in bacteria, a comparable penetration ability has been reported for *Streptomyces* sp. SCUT-
577 3 during feather degradation [15], suggesting that physical substrate invasion may also
578 complement enzymatic degradation in filamentous bacteria such as strain G11C. Overall, the
579 characteristic mycelial growth of *Streptomyces*, distinct from that of keratinolytic bacteria such as
580 *Bacillus* [95] and *Pseudomonas* [96], appears to contribute substantially to feather degradation by
581 facilitating substrate colonization, adhesion, and localized enzyme secretion.

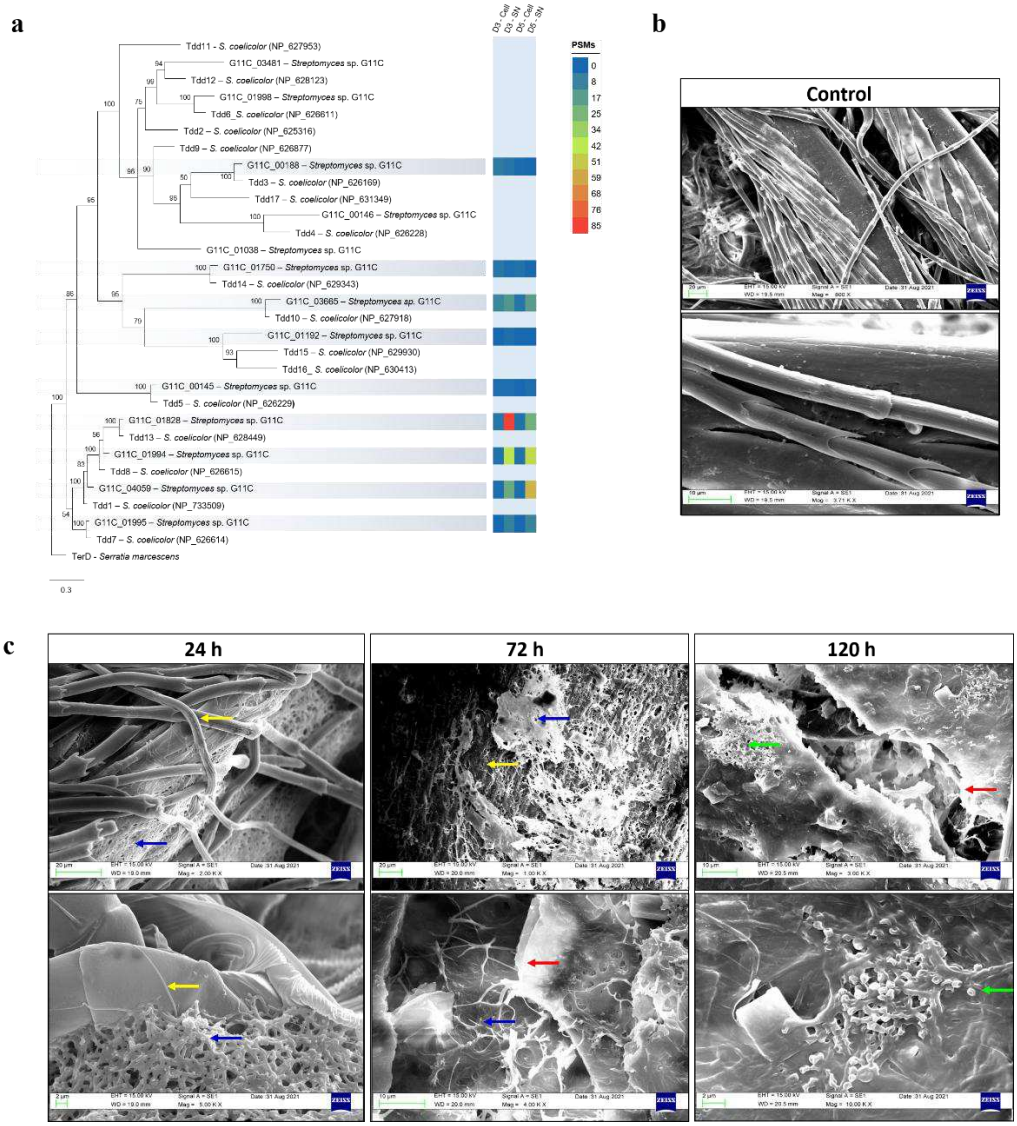


Figure 5. Phylogenetic relationships of TerD proteins and structural dynamics of feather degradation by *Streptomyces* sp. G11C. (a) Maximum-likelihood phylogenetic tree of TerD homologs encoded in the G11C genome and previously characterized Tdd proteins from *Streptomyces coelicolor*. The heatmap shows total PSMs detected in cellular (Cell) and extracellular (SN) fractions after 3 and 5 days of growth on feathers. (b) Scanning electron microscopy (SEM) micrographs of native feather structure (c) SEM analysis of feather degradation after 24, 72, and 120 h of culture with strain G11C. Colored arrows indicate feather structures and degradation-associated features: barbules (yellow), mycelium (blue), spores (green), and surface slits (red).

Updated model of the keratin degradation mechanism mediated by *Streptomyces* sp. G11C

Recent omics studies in keratinolytic bacteria, including *Streptomyces*, *Bacillus*, and *Pseudomonas*, have highlighted keratin degradation as a complex, multicomponent process involving redox systems, sulfur metabolism, peptide transport, and diverse proteolytic enzymes acting synergistically [13,15,41,56,68,77]. Consistent with this view, the combined proteomic, physiological, and microscopic evidence obtained for *Streptomyces* sp. G11C expands our previous model of feather degradation [20], revealing that the process involves not only keratinase-mediated hydrolysis but also keratin denaturation, disulfide bond reduction, substrate colonization, peptide assimilation, and cellular stress responses.

In this model (Figure 6), degradation begins with mycelial colonization of the feather surface (process I), enabling localized secretion of extracellular enzymes that target disulfide bonds, glycosylated regions, and peptide bonds, initiating keratin denaturation. Structural destabilization proceeds through complementary oxidative and reductive mechanisms (process II). Oxidative modification of glycosylated regions, mediated by lytic polysaccharide monooxygenases (LPMOs such as G11C_02990, G11C_02174, G11C_03647 and G11C_01517), likely induces conformational changes in the keratin filament network, increasing accessibility of proteolytic enzymes. In parallel, reductive cleavage of intermolecular disulfide bonds may be driven primarily by dihydrolipoyl dehydrogenases (G11C_04958 and G11C_02220) and reinforced by additional redox systems, including glutathione metabolism mediated by γ-glutamyl transferase (GGT; G11C_03747), which generates cysteinyl-containing reducing equivalents, and by sulfite-mediated sulfitolysis (process V). Following partial destabilization, extracellular keratinolytic proteases gain access to the substrate and initiate extensive peptide bond hydrolysis (process III). This step involves serine endoproteases from families S8 and S1 (G11C_03013, G11C_05151, and G11C_01510) together with metalloproteases (G11C_02936), whose activity is

615 complemented by exoproteases such as aminopeptidases (G11C_00115, G11C_05004),
616 carboxypeptidases (G11C_04917, G11C_03659), and oligopeptidases (G11C_04461,
617 G11C_03907) that further process peptide fragments into smaller oligopeptides and amino acids
618 (process IV). The resulting peptides and amino acids are subsequently imported through peptide
619 transport systems (process VI), including ABC transporters (G11C_03026 and G11C_00116) and
620 MFS transporter (G11C_03897 and G11C_05075), and further processed by intracellular
621 peptidases such as aminopeptidase N (G11C_05149) and leucyl aminopeptidase (G11C_00115).
622 These metabolites then enter central metabolic pathways, supplying carbon, nitrogen, and sulfur
623 to support cellular growth. Keratin-derived peptides may also contribute to the induction of
624 keratinolytic enzyme expression, thereby promoting their transcription and translation, whereas
625 chaperones such as DnaK (G11C_03178) may assist in the folding and stabilization of newly
626 synthesized enzymes (process VII). Simultaneously, growth on keratin-rich substrates appears
627 coupled to physiological adaptation mechanisms. Redox homeostasis and oxidative stress
628 management (process VIII) are supported by catalases (G11C_01735, and G11C_01953),
629 superoxide dismutases (G11C_00771 and G11C_02009), and thioredoxin-related proteins
630 (G11C_02846, G11C_02847, G11C_03466). Proteins related to morphological differentiation and
631 calcium homeostasis, including TerD homologs (G11C_01828, G11C_01994, G11C_04059),
632 together with cell wall-remodeling enzymes such as lysozyme (G11C_02544) and peptidoglycan-
633 associated metallopeptidases of families M23 (G11C_00564) and M15 (G11C_04917,
634 G11C_04461), suggest that developmental transitions and controlled cell lysis may contribute to
635 enzyme release and nutrient recycling within the mycelial network (process IX). Altogether, this
636 model describes feather keratin degradation by *Streptomyces* sp. G11C as a coordinated process

involving keratin destabilization, extracellular proteolysis, peptide assimilation, and physiological adaptation, ultimately enabling efficient utilization of this highly recalcitrant protein substrate.

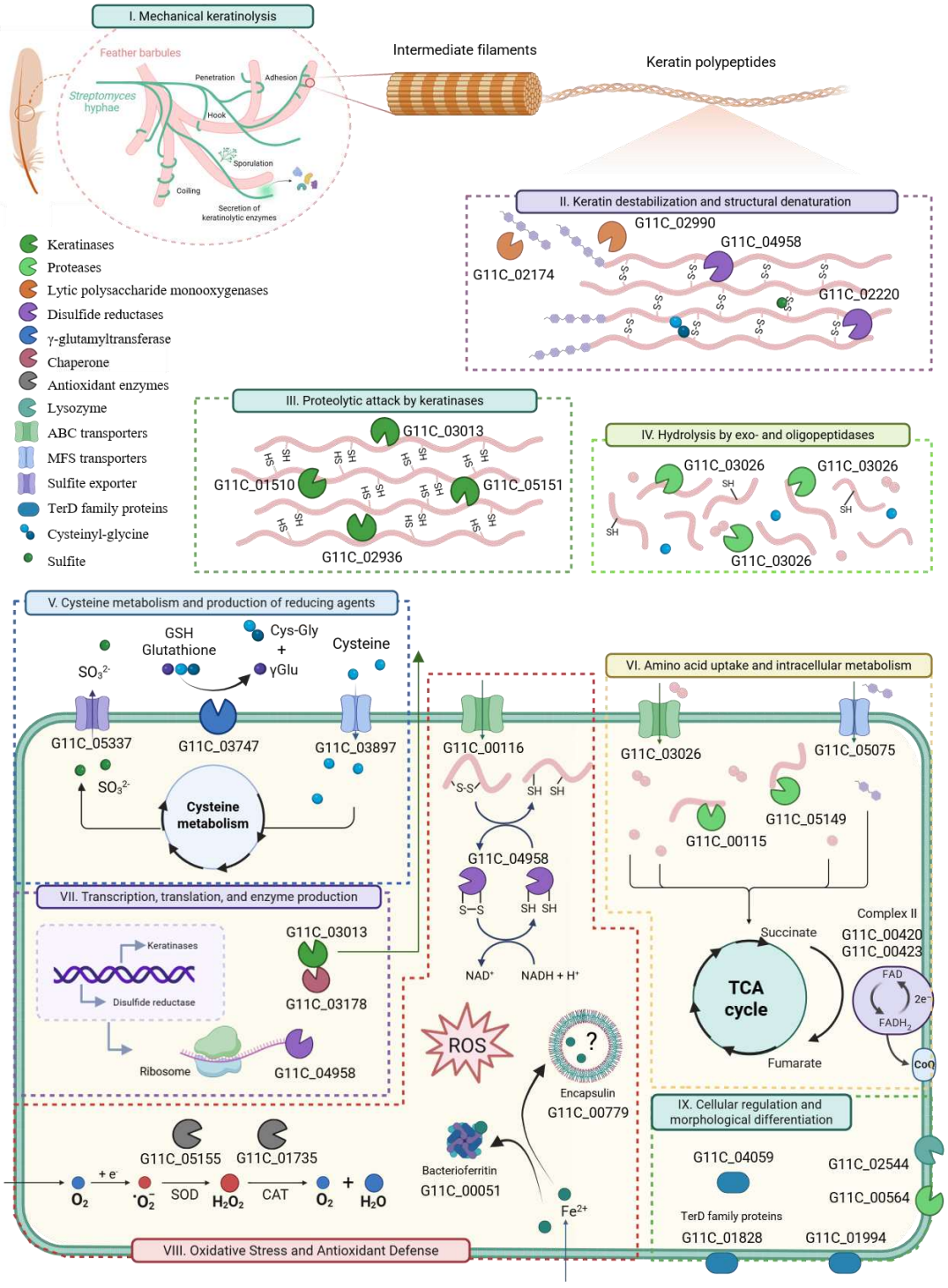


Figure 6. Proposed model of feather keratin degradation mechanism mediated by *Streptomyces* sp. G11C. The model depicts the main processes involved, including mechanical keratinolysis and substrate colonization (I), keratin destabilization and structural denaturation (II), proteolytic attack by keratinases (III), peptide hydrolysis by exo- and oligopeptidases (IV), cysteine metabolism and production of reducing agents (V), amino acid uptake and intracellular metabolism (VI), transcription, translation, and enzyme production (VII), oxidative stress and antioxidant defense (VIII), and cellular regulation and morphological differentiation (IX). Arrows reflect proposed functional relationships based on protein representation, subcellular localization predictions, and literature on related systems; several steps remain hypothetical and require experimental validation in strain G11C. This figure was created using BioRender.com.

Conclusions

This study provides new insights into the molecular mechanisms underlying feather keratin degradation by *Streptomyces* sp. G11C. Temporal proteomic analysis revealed that keratin utilization involves coordinated processes that extend beyond extracellular proteolysis, including redox-mediated destabilization of the keratin matrix, oxidative remodeling, peptide assimilation, and cellular adaptation to growth on recalcitrant protein substrates. Our results highlight oxidoreductases as key contributors to keratin denaturation. In particular, the high abundance of dihydrolipoyl dehydrogenase suggests that this enzyme may participate in the reductive cleavage of keratin disulfide bonds, representing a mechanism not previously reported in keratinolytic microorganisms. Additional redox systems, including γ-glutamyl transferase–mediated glutathione metabolism and sulfite production, may further contribute to disulfide bond reduction, while the presence of lytic polysaccharide monooxygenases likely contribute to oxidative modifications that enhance substrate accessibility. Importantly, the temporal dynamics observed between early (day 3) and later (day 5) stages indicate that keratin degradation is a dynamic and progressive process, with initial stages dominated by substrate colonization and redox-mediated

665 destabilization, followed by extensive proteolysis, peptide assimilation, and metabolic utilization
666 of keratin-derived nutrients. This temporal specialization underscores the adaptability of
667 *Streptomyces* sp. G11C and highlights the importance of time-resolved analyses to fully capture
668 the complexity of keratin degradation processes. Consistent with this model, overexpression of S8
669 and M6 proteases increased keratinolytic activity, confirming their direct contribution to substrate
670 degradation. Altogether, these findings support an updated model of keratin degradation in which
671 proteolytic activity operates in concert with redox-driven mechanisms and cellular adaptation
672 processes, enabling efficient utilization of feather keratin and highlighting oxidoreductase-
673 mediated reactions as previously underappreciated components of microbial keratin degradation.
674
675 **Supplementary Information**
676 **Table S1.** Raw data of proteins identified in each sample from the proteomic analysis (XLSX file)
677 **Table S2.** TerD homologs from *Streptomyces coelicolor* A3(2) used for phylogenetic analysis
678 (PDF)
679 **Table S3.** List of the most abundant proteins detected across samples (PDF)
680 **Table S4.** Candidate proteins supporting the proposed model of feather keratin degradation by
681 *Streptomyces* sp. G11C (PDF)
682 **Figure S1.** Antioxidant and ROS defense mechanisms potentially involved in feather degradation
683 by *Streptomyces* sp. G11C (PDF)
684
685 **Abbreviations**
686 PSMs: peptide-spectrum matches; LPMOs: lytic polysaccharide monooxygenases; SH: sulfhydryl
687 groups; NH: amino groups; COGs: Clusters of Orthologous Groups; FDR: false discovery rate;

GSSG: oxidized glutathione; GGT: γ-glutamyl transferase; LC-MS/MS: liquid chromatography–tandem mass spectrometry.

Acknowledgment

The proteomic analysis was performed at the Proteomics Core Facility, Sahlgrenska academy, Gothenburg University, with financial support from SciLifeLab and BioMS.

Author Contributions

VG, MJVS, AU and BC contributed to the conception and design of the experiments. VG and NSC performed the experiments. RK and LA performed the proteomic analysis and protein identification. VG, and MJVS analyzed the data. VG and MJVS wrote and edited the manuscript. All authors contributed to manuscript revision, read and approved the submitted version. All authors have given approval to the final version of the manuscript.

Funding Sources

Financial support was provided by the Agencia Nacional de Investigación y Desarrollo (ANID), with projects: Fondecyt postdoctoral project N°3230679 (VG), Postdoctoral USM2025 (NS), Fondecyt regular Nº1221264 (BC), and Millenium Nucleus BioGEM NCN_2023_054 (BC, VG, NS, MS).

Data availability

All data generated during this study are included in this published article and its additional files.

Declarations

Ethical approval

Not applicable.

Consent to participate

Not applicable.

Informed consent

Not applicable.

Consent for publication

All authors have read and agreed to the published version of the manuscript.

Competing interests

The authors declare no competing interests.

References

(1) Organisation for Economic Co-operation and Development (OECD); Food and Agriculture Organization of the United Nations (FAO). *OECD-FAO Agricultural Outlook 2025-2034*; OECD-FAO Agricultural Outlook; OECD Publishing, 2025. https://www.oecd.org/en/publications/oecd-fao-agricultural-outlook-2025-2034_601276cd-en.html.

(2) Lai, Y.; Wu, X.; zheng, X.; Li, W.; Wang, L. Insights into the Keratin Efficient Degradation Mechanism Mediated by Bacillus Sp. CN2 Based on Integrating Functional Degradomics. *Biotechnology for Biofuels and Bioproducts* **2023**, *16* (1), 1–14. https://doi.org/10.1186/s13068-023-02308-0.

(3) Park, G.; Lee, K. M.; Lee, Y. S.; Kim, Y.; Jeon, C. M.; Lee, O. M.; Kim, Y. J.; Son, H. J. Biodegradation and Valorization of Feather Waste Using the Keratinase-Producing Bacteria and Their Application in Environmentally Hazardous Industrial Processes. *J. Environ. Manage.* **2023**, *346*, 118986. https://doi.org/10.1016/j.jenvman.2023.118986.

(4) Anbesaw, M. S. Bioconversion of Keratin Wastes Using Keratinolytic Microorganisms to Generate Value-Added Products. *Int. J. Biomater.* **2022**, *2022* (1), 2048031. https://doi.org/10.1155/2022/2048031.

(5) Chen, H.; Gao, S.; Li, Y.; Xu, H. J.; Li, W.; Wang, J.; Zhang, Y. Valorization of Livestock Keratin Waste: Application in Agricultural Fields. *Int. J. Environ. Res. Public Health* **2022**, *19* (11), 6681. https://doi.org/10.3390/ijerph19116681.

(6) Feroz, S.; Muhammad, N.; Ranayake, J.; Dias, G. Keratin - Based Materials for Biomedical Applications. *Bioact. Mater.* **2020**, *5* (3), 496–509. https://doi.org/10.1016/j.bioactmat.2020.04.007.

(7) Shavandi, A.; Silva, T. H.; Bekhit, A. A.; Bekhit, A. E. D. A. Keratin: Dissolution, Extraction and Biomedical Application. *Biomater. Sci.* **2017**, *5* (9), 1699–1735. https://doi.org/10.1039/c7bm00411g.

(8) Song, C.; Liu, R.; Yin, D.; Xie, C.; Liang, Y.; Yang, D.; Jiang, M.; Zhang, H.; Shen, N. A Comparative Transcriptome Analysis Unveils the Mechanisms of Response in Feather Degradation by Pseudomonas Aeruginosa Gxun-7. *Microorganisms* **2024**, *12* (4), 841. https://doi.org/10.3390/microorganisms12040841.

(9) Li, Q. Structure, Application, and Biochemistry of Microbial Keratinases. *Front. Microbiol.* **2021**, *12*, 674345. https://doi.org/10.3389/fmicb.2021.674345.

(10) Qiu, J.; Wilkens, C.; Barrett, K.; Meyer, A. S. Microbial Enzymes Catalyzing Keratin Degradation: Classification, Structure, Function. *Biotechnol. Adv.* **2020**, *44*, 107607. https://doi.org/10.1016/j.biotechadv.2020.107607.

(11) Peng, Z.; Zhang, J.; Du, G.; Chen, J. Keratin Waste Recycling Based on Microbial Degradation: Mechanisms and Prospects. *ACS Sustain. Chem. Eng.* **2019**, *7* (11), 9727–9736. https://doi.org/10.1021/acssuschemeng.9b01527.

(12) Lange, L.; Huang, Y.; Busk, P. K. Microbial Decomposition of Keratin in Nature—a New Hypothesis of Industrial Relevance. *Appl. Microbiol. Biotechnol.* **2016**, *100* (5), 2083–2096. https://doi.org/10.1007/s00253-015-7262-1.

(13) Huang, Y.; Łężyk, M.; Herbst, F. A.; Busk, P. K.; Lange, L. Novel Keratinolytic Enzymes, Discovered from a Talented and Efficient Bacterial Keratin Degrader. *Sci. Rep.* **2020**, *10* (1), 10033. https://doi.org/10.1038/s41598-020-66792-2.

(14) Liu, Q.; Zhang, T.; Song, N.; Li, Q.; Wang, Z.; Zhang, X.; Lu, X.; Fang, J.; Chen, J. Purification and Characterization of Four Key Enzymes from a Feather-Degrading Bacillus

Subtilis from the Gut of Tarantula Chilobrachys Guangxiensis. *Int. Biodeterior. Biodegradation* **2014**, *96*, 26–32. https://doi.org/10.1016/j.ibiod.2014.08.008.

(15) Li, Z. W.; Liang, S.; Ke, Y.; Deng, J. J.; Zhang, M. S.; Lu, D. L.; Li, J. Z.; Luo, X. C. The Feather Degradation Mechanisms of a New Streptomyces Sp. Isolate SCUT-3. *Commun. Biol.* **2020**, *3* (1), 191. https://doi.org/10.1038/s42003-020-0918-0.

(16) Rahayu, S.; Syah, D.; Thenawidjaja Suhartono, M. Degradation of Keratin by Keratinase and Disulfide Reductase from Bacillus Sp. MTS of Indonesian Origin. *Biocatal. Agric. Biotechnol.* **2012**, *1* (2), 152–158. https://doi.org/10.1016/j.bcab.2012.02.001.

(17) Böckle, B.; Müller, R. Reduction of Disulfide Bonds by Streptomyces Pactum during Growth on Chicken Feathers. *Appl. Environ. Microbiol.* **1997**, *63* (2), 790–792. https://doi.org/10.1128/aem.63.2.790-792.1997.

(18) Pavale, S.; Isembart, C.; Shapaval, V.; Tuveng, T. R.; Rosa, S. L. La; Eijsink, V. G. H. Proteolytic and Non-Proteolytic Mechanisms of Keratin Degradation in Onygena Corvina Revealed by a Proteogenomic Approach. *Appl. Environ. Microbiol.* **2025**, *91* (12), e01727-25. https://doi.org/10.1128/aem.01727-25.

(19) Wang, Z.; Chen, Y.; Yan, M.; Li, K.; Okoye, C. O.; Fang, Z.; Ni, Z.; Chen, H. Research Progress on the Degradation Mechanism and Modification of Keratinase. *Appl. Microbiol. Biotechnol.* **2023**, *107* (4), 1003–1017. https://doi.org/10.1007/s00253-023-12360-3.

(20) González, V.; Vargas-Straube, M. J.; Beys-Da-Silva, W. O.; Santi, L.; Valencia, P.; Beltrametti, F.; Cámara, B. Enzyme Bioprospection of Marine-Derived Actinobacteria from the Chilean Coast and New Insight in the Mechanism of Keratin Degradation in

794 Streptomyces Sp. G11C. *Mar. Drugs* **2020**, *18* (11), 537.
795 https://doi.org/10.3390/MD18110537.

796 (21) Nielsen, P. M.; Petersen, D.; Dambmann, C. Improved Method for Determining Food
797 Protein Degree of Hydrolysis. *J. Food Sci.* **2001**, *66*, 642–646.

798 (22) Ellman, G. L. Tissue Sulfhydryl Groups. *Arch. Biochem. Biophys.* **1959**, *82*, 70–77.

799 (23) Bradford, M. M. A Rapid and Sensitive Method for the Quantification of Microgram
800 Quantities of Protein Utilizing the Principle of Protein-Dye Binding. *Anal. Biochem.* **1976**,
801 *72*, 248–254. https://doi.org/10.1016/j.cj.2017.04.003.

802 (24) Huang, Y.; Busk, P. K.; Herbst, F. A.; Lange, L. Genome and Secretome Analyses Provide
803 Insights into Keratin Decomposition by Novel Proteases from the Non-Pathogenic Fungus
804 Onygena Corvina. *Appl. Microbiol. Biotechnol.* **2015**, *99* (22), 9635–9649.
805 https://doi.org/10.1007/s00253-015-6805-9.

806 (25) Valencia, R.; González, V.; Undabarrena, A.; Zamora-Leiva, L.; Ugalde, J. A.; Cámara, B.
807 An Integrative Bioinformatic Analysis for Keratinase Detection in Marine-Derived
808 Streptomyces. *Mar. Drugs* **2021**, *19* (6), 286. https://doi.org/10.3390/md19060286.

809 (26) Kito, K.; Ito, T. Mass Spectrometry-Based Approaches Toward Absolute Quantitative
810 Proteomics. *Curr. Genomics* **2008**, *9* (4), 263–274.
811 https://doi.org/10.2174/138920208784533647.

812 (27) Batra, V.; Dagar, K.; Diwakar, M. P.; Kumaresan, A.; Kumar, R.; Datta, T. K. The
813 Proteomic Landscape of Sperm Surface Deciphers Its Maturational and Functional Aspects

in Buffalo. *Front. Physiol.* **2024**, *15*, 1413817. https://doi.org/10.3389/fphys.2024.1413817.

(28) Sanchez, G.; Yu, C.-S.; Chen, Y.-C.; Lu, C.-H.; Hwang, J.-K. Prediction of Protein Subcellular Localization. *PROTEINS: Structure, Function, and Bioinformatics* **2006**, *64*, 643–651. https://doi.org/10.1002/prot.

(29) Almagro Armenteros, J. J.; Tsirigos, K. D.; Sønderby, C. K.; Petersen, T. N.; Winther, O.; Brunak, S.; von Heijne, G.; Nielsen, H. SignalP 5.0 Improves Signal Peptide Predictions Using Deep Neural Networks. *Nat. Biotechnol.* **2019**, *37* (4), 420–423. https://doi.org/10.1038/s41587-019-0036-z.

(30) Huerta-Cepas, J.; Szklarczyk, D.; Heller, D.; Hernández-Plaza, A.; Forslund, S. K.; Cook, H.; Mende, D. R.; Letunic, I.; Rattei, T.; Jensen, L. J.; Von Mering, C.; Bork, P. EggNOG 5.0: A Hierarchical, Functionally and Phylogenetically Annotated Orthology Resource Based on 5090 Organisms and 2502 Viruses. *Nucleic Acids Res.* **2019**, *47* (D1), D309–D314. https://doi.org/10.1093/nar/gky1085.

(31) Chen, C.; Chen, H.; Zhang, Y.; Thomas, H. R.; Frank, M. H.; He, Y.; Xia, R. TBtools: An Integrative Toolkit Developed for Interactive Analyses of Big Biological Data. *Mol. Plant* **2020**, *13* (8), 1194–1202. https://doi.org/10.1016/j.molp.2020.06.009.

(32) Katoh, K.; Standley, D. M. MAFFT Multiple Sequence Alignment Software Version 7: Improvements in Performance and Usability. *Mol. Biol. Evol.* **2013**, *30* (4), 772–780. https://doi.org/10.1093/molbev/mst010.

(33) Larsson, A. AliView: A Fast and Lightweight Alignment Viewer and Editor for Large Datasets. *Bioinformatics* **2014**, *30* (22), 3276–3278. https://doi.org/10.1093/bioinformatics/btu531.

(34) Ronquist, F.; Teslenko, M.; Van Der Mark, P.; Ayres, D. L.; Darling, A.; Höhna, S.; Larget, B.; Liu, L.; Suchard, M. A.; Huelsenbeck, J. P. Mrbayes 3.2: Efficient Bayesian Phylogenetic Inference and Model Choice across a Large Model Space. *Syst. Biol.* **2012**, *61* (3), 539–542. https://doi.org/10.1093/sysbio/sys029.

(35) Letunic, I.; Bork, P. Interactive Tree of Life (ITOL) v5: An Online Tool for Phylogenetic Tree Display and Annotation. *Nucleic Acids Res.* **2021**, *49* (W1), W293–W296. https://doi.org/10.1093/nar/gkab301.

(36) Ramnani, P.; Singh, R.; Gupta, R. Keratinolytic Potential of Bacillus Licheniformis RG1: Structural and Biochemical Mechanism of Feather Degradation. *Can. J. Microbiol.* **2005**, *51* (3), 191–196. https://doi.org/10.1139/w04-123.

(37) Montes, C.; Vélez, J. H.; Ramírez, G.; Isaacs, M.; Arce, R.; Aguirre, M. J. Critical Comparison between Modified Monier-Williams and Electrochemical Methods to Determine Sulfite in Aqueous Solutions. *The Scientific World Journal* **2012**, *2012* (2), 0–5. https://doi.org/10.1100/2012/168148.

(38) Bibb, M. J.; Janssen, G. R.; Ward, J. M. Cloning and Analysis of the Promoter Region of the Erythromycin Resistance Gene (ErmE) of Streptomyces Erythraeus. *Gene* **1985**, *38* (1–3), 215–226. https://doi.org/10.1016/0378-1119(85)90220-3.

(39) Flett, F.; Mersinias, V.; Smith, C. P. High Efficiency Intergeneric Conjugal Transfer of Plasmid DNA from Escherichia Coli to Methyl DNA-Restricting Streptomycetes. *FEMS Microbiol. Lett.* **2006**, *155* (2), 223–229. https://doi.org/10.1111/j.1574-6968.1997.tb13882.x.

(40) Mitteer, D. R.; Greer, B. D.; Fisher, W. W.; Cohrs, V. L. Teaching Behavior Technicians to Create Publication-Quality, Single-Case Design Graphs in Graphpad Prism 7. *J. Appl. Behav. Anal.* **2018**, *9999*, 1–13. https://doi.org/10.1002/jaba.483.

(41) Javier-López, R.; Kielbasa, M.; Armengaud, J.; Birkeland, N. K. Transcriptomic and Proteomic Insights into Feather Keratin Degradation by Fervidobacterium. *Front. Microbiol.* **2025**, *16*, 1509937. https://doi.org/10.3389/fmicb.2025.1509937.

(42) Srinivasan, S. R.; Gillies, A. T.; Chang, L.; Thompson, A. D.; Gestwicki, J. E. Molecular Chaperones DnaK and DnaJ Share Predicted Binding Sites on Most Proteins in the E. Coli Proteome. *Mol. Biosyst.* **2012**, *8* (9), 2323–2333. https://doi.org/10.1039/c2mb25145k.

(43) Almeida, A. V.; Carvalho, A. J.; Pereira, A. S. Encapsulin Nanocages: Protein Encapsulation and Iron Sequestration. *Coord. Chem. Rev.* **2021**, *448*, 214188. https://doi.org/10.1016/j.ccr.2021.214188.

(44) Anantharaman, V.; Iyer, L. M.; Aravind, L. Ter-Dependent Stress Response Systems: Novel Pathways Related to Metal Sensing, Production of a Nucleoside-like Metabolite, and DNA-Processing. *Mol. Biosyst.* **2012**, *8* (12), 3142–3165. https://doi.org/10.1039/c2mb25239b.

(45) Manteca, A.; Mäder, U.; Connolly, B. A.; Sanchez, J. A Proteomic Analysis of Streptomyces Coelicolor Programmed Cell Death. *Proteomics* **2006**, *6* (22), 6008–6022. https://doi.org/10.1002/pmic.200600147.

(46) Faddetta, T.; Renzone, G.; Vassallo, A.; Rimini, E.; Nasillo, G.; Buscarino, G.; Agnello, S.; Licciardi, M.; Botta, L.; Scaloni, A.; Piccionello, A. P.; Puglia, A. M.; Gallo, G. Streptomyces Coelicolor Vesicles: Many Molecules to Be Delivered. *Appl. Environ. Microbiol.* **2022**, *88* (1), e01881-21. https://doi.org/10.1128/AEM.01881-21.

(47) Meyer, K. J.; Nodwell, J. R. Streptomyces Extracellular Vesicles Are a Broad and Permissive Antimicrobial Packaging and Delivery System. *J. Bacteriol.* **2024**, *206* (3), e00325-23. https://doi.org/10.1128/jb.00325-23.

(48) Matamouros, S.; Gensch, T.; Cerff, M.; Sachs, C. C.; Abdollahzadeh, I.; Hendriks, J.; Horst, L.; Tenhaef, N.; Tenhaef, J.; Noack, S.; Graf, M.; Takors, R.; Nöh, K.; Bott, M. Growth-Rate Dependency of Ribosome Abundance and Translation Elongation Rate in Corynebacterium Glutamicum Differs from That in Escherichia Coli. *Nat. Commun.* **2023**, *14* (1), 5611. https://doi.org/10.1038/s41467-023-41176-y.

(49) Anjou, C.; Lotoux, A.; Morvan, C.; Martin-Verstraete, I. From Ubiquity to Specificity: The Diverse Functions of Bacterial Thioredoxin Systems. *Environ. Microbiol.* **2024**, *26* (6), e16668. https://doi.org/10.1111/1462-2920.16668.

(50) Si, M.; Wang, J.; Xiao, X.; Guan, J.; Zhang, Y.; Ding, W.; Chaudhry, M. T.; Wang, Y.; Shen, X. Ohr Protects Corynebacterium Glutamicum against Organic Hydroperoxide Induced Oxidative Stress. *PLoS One* **2015**, *10* (6), e0131634. https://doi.org/10.1371/journal.pone.0131634.

(51) Martínez-Antonio, A.; Collado-Vides, J. Identifying Global Regulators in Transcriptional Regulatory Networks in Bacteria. *Curr. Opin. Microbiol.* **2003**, *6* (5), 482–489. https://doi.org/10.1016/j.mib.2003.09.002.

(52) Sedláček, V.; Kučera, I. Modifications of the Aerobic Respiratory Chain of Paracoccus Denitrificans in Response to Superoxide Oxidative Stress. *Microorganisms* **2019**, *7* (12), 740. https://doi.org/10.3390/microorganisms7120640.

(53) Gupta, R.; Ramnani, P. Microbial Keratinases and Their Prospective Applications: An Overview. *Appl. Microbiol. Biotechnol.* **2006**, *70* (1), 21–33. https://doi.org/10.1007/s00253-005-0239-8.

(54) Sharma, R.; Gupta, R. Coupled Action of γ-Glutamyl Transpeptidase-Glutathione and Keratinase Effectively Degrades Feather Keratin and Surrogate Prion Protein, Sup 35NM. *Bioresour. Technol.* **2012**, *120*, 314–317. https://doi.org/10.1016/j.biortech.2012.06.038.

(55) He, Z.; Sun, R.; Tang, Z.; Bu, T.; Wu, Q.; Li, C.; Chen, H. Biodegradation of Feather Waste Keratin by the Keratin-Degrading Strain Bacillus Subtilis 8. *J. Microbiol. Biotechnol.* **2018**, *28* (2), 314–322. https://doi.org/10.4014/jmb.1708.08077.

(56) Lai, Y.; Wu, X.; zheng, X.; Li, W.; Wang, L. Insights into the Keratin Efficient Degradation Mechanism Mediated by Bacillus Sp. CN2 Based on Integrating Functional Degradomics. *Biotechnology for Biofuels and Bioproducts* **2023**, *16* (1), 59. https://doi.org/10.1186/s13068-023-02308-0.

(57) Grumbt, M.; Monod, M.; Yamada, T.; Hertweck, C.; Kunert, J.; Staib, P. Keratin Degradation by Dermatophytes Relies on Cysteine Dioxygenase and a Sulfite Efflux Pump.

916 *Journal of Investigative Dermatology* **2013**, *133* (6), 1550–1555.
917 https://doi.org/10.1038/jid.2013.41.

918 (58) Peng, Z.; Xu, P.; Song, Y.; Du, G.; Zhang, J.; Chen, J. Cysteine-Mediated Cyclic
919 Metabolism Drives the Microbial Degradation of Keratin. *ACS Sustain. Chem. Eng.* **2021**,
920 *9* (29), 9861–9870. https://doi.org/10.1021/acssuschemeng.1c02627.

921 (59) Newton, G. L.; Buchmeier, N.; Fahey, R. C. Biosynthesis and Functions of Mycothiol, the
922 Unique Protective Thiol of Actinobacteria. *Microbiology and Molecular Biology Reviews*
923 **2008**, *72* (3), 471–494. https://doi.org/10.1128/mmbr.00008-08.

924 (60) Jothivasan, V. K.; Hamilton, C. J. Mycothiol: Synthesis, Biosynthesis and Biological
925 Functions of the Major Low Molecular Weight Thiol in Actinomycetes. *Nat. Prod. Rep.*
926 **2008**, *25* (6), 1091–1117. https://doi.org/10.1039/b616489g.

927 (61) Fang, Z.; Zhang, J.; Liu, B.; Du, G.; Chen, J. Biochemical Characterization of Three
928 Keratinolytic Enzymes from Stenotrophomonas Maltophilia BBE11-1 for Biodegrading
929 Keratin Wastes. *Int. Biodeterior. Biodegradation* **2013**, *82*, 166–172.
930 https://doi.org/10.1016/j.ibiod.2013.03.008.

931 (62) Prakash, P.; Jayalakshmi, S. K.; Sreeramulu, K. Purification and Characterization of
932 Extreme Alkaline, Thermostable Keratinase, and Keratin Disulfide Reductase Produced by
933 Bacillus Halodurans PPKS-2. *Appl. Microbiol. Biotechnol.* **2010**, *87* (2), 625–633.
934 https://doi.org/10.1007/s00253-010-2499-1.

(63) Yamamura, S.; Morita, Y.; Hasan, Q.; Yokoyama, K.; Tamiya, E. Keratin Degradation: A Cooperative Action of Two Enzymes from Stenotrophomonas Sp. *Biochem. Biophys. Res. Commun.* **2002**, *294* (5), 1138–1143. https://doi.org/10.1016/S0006-291X(02)00580-6.

(64) De Kok, A.; Hengeveld, A. F.; Martin, A.; Westphal, A. H. The Pyruvate Dehydrogenase Multi-Enzyme Complex from Gram-Negative Bacteria. *Biochimica et Biophysica Acta - Protein Structure and Molecular Enzymology* **1998**, *1385* (2), 353–366. https://doi.org/10.1016/S0167-4838(98)00079-X.

(65) Forsberg, Z.; Sørlie, M.; Petrović, D.; Courtade, G.; Aachmann, F. L.; Vaaje-Kolstad, G.; Bissaro, B.; Røhr, Å. K.; Eijsink, V. G. Polysaccharide Degradation by Lytic Polysaccharide Monooxygenases. *Curr. Opin. Struct. Biol.* **2019**, *59*, 54–64. https://doi.org/10.1016/j.sbi.2019.02.015.

(66) Li, F.; Zhao, H.; Liu, Y.; Zhang, J.; Yu, H. Chitin Biodegradation by Lytic Polysaccharide Monooxygenases from Streptomyces Coelicolor In Vitro and In Vivo. *Int. J. Mol. Sci.* **2023**, *24* (1), 275. https://doi.org/10.3390/ijms24010275.

(67) Rawlings, N. D.; Waller, M.; Barrett, A. J.; Bateman, A. MEROPS: The Database of Proteolytic Enzymes, Their Substrates and Inhibitors. *Nucleic Acids Res.* **2014**, *42* (D1), D503–D509. https://doi.org/10.1093/nar/gkt953.

(68) Zhou, B.; Guo, Y.; Xue, Y.; Ji, X.; Huang, Y. Comprehensive Insights into the Mechanism of Keratin Degradation and Exploitation of Keratinase to Enhance the Bioaccessibility of Soybean Protein. *Biotechnology for Biofuels and Bioproducts* **2023**, *16* (1), 177. https://doi.org/10.1186/s13068-023-02426-9.

(69) Han, S.; Lu, Y.; Peng, L.; Dong, X.; Zhu, L.; Han, Y. Transcriptomics Reveals the Mechanism of Purpureocillium Lilacinum GZAC18-2JMP in Degrading Keratin Material. *Curr. Microbiol.* **2024**, *81* (8), 227. https://doi.org/10.1007/s00284-024-03757-y.

(70) Vikash, V. L.; Kamini, N. R.; Ponesakki, G.; Anandasadagopan, S. K. Keratinous Bioresources: Their Generation, Microbial Degradation, and Value Enhancement for Biotechnological Applications. *World J. Microbiol. Biotechnol.* **2025**, *41* (4), 118. https://doi.org/10.1007/s11274-025-04336-4.

(71) Dalhammar, G.; Steiner, H. Characterization of Inhibitor A, a Protease from Bacillus Thuringiensis Which Degrades Attacins and Cecropins, Two Classes of Antibacterial Proteins in Insects. *Eur. J. Biochem.* **1984**, *139* (2), 247–252. https://doi.org/10.1111/j.1432-1033.1984.tb08000.x.

(72) Lövgren, A.; Zhang, M.; Engström, A.; Dalhammar, G.; Landén, R. Molecular Characterization of Immune Inhibitor A, a Secreted Virulence Protease from Bacillus Thuringiensis. *Mol. Microbiol.* **1990**, *4* (12), 2137–2146. https://doi.org/10.1111/j.1365-2958.1990.tb00575.x.

(73) Arima, J.; Uesugi, Y.; Iwabuchi, M.; Hatanaka, T. Alteration of Leucine Aminopeptidase from Streptomyces Septatus TH-2 to Phenylalanine Aminopeptidase by Site-Directed Mutagenesis. *Appl. Environ. Microbiol.* **2005**, *71* (11), 7229–7235. https://doi.org/10.1128/AEM.71.11.7229-7235.2005.

(74) Addlagatta, A.; Gay, L.; Matthews, B. W. Structure of Aminopeptidase N from Escherichia Coli Suggests a Compartmentalized, Gated Active Site. *Proc. Natl. Acad. Sci. U. S. A.* **2006**, *103* (36), 13339–13344. https://doi.org/10.1073/pnas.0606167103.

(75) Yu, J.; Ge, J.; Heuveling, J.; Schneider, E.; Yang, M. Structural Basis for Substrate Specificity of an Amino Acid ABC Transporter. *Proc. Natl. Acad. Sci. U. S. A.* **2015**, *112* (16), 5243–5248. https://doi.org/10.1073/pnas.1415037112.

(76) Zhang, X. C.; Zhao, Y.; Heng, J.; Jiang, D. Energy Coupling Mechanisms of MFS Transporters. *Protein Science* **2015**, *24* (10), 1560–1579. https://doi.org/10.1002/pro.2759.

(77) Song, C.; Liu, R.; Yin, D.; Xie, C.; Liang, Y.; Yang, D.; Jiang, M.; Zhang, H.; Shen, N. A Comparative Transcriptome Analysis Unveils the Mechanisms of Response in Feather Degradation by Pseudomonas Aeruginosa Gxun-7. *Microorganisms* **2024**, *12* (4), 841. https://doi.org/10.3390/microorganisms12040841.

(78) Schirawski, J.; Unden, G. Menaquinone-Dependent Succinate Dehydrogenase of Bacteria Catalyzes Reversed Electron Transport Driven by the Proton Potential. *Eur. J. Biochem.* **1998**, *257* (1), 210–215. https://doi.org/10.1046/j.1432-1327.1998.2570210.x.

(79) Shiota, Y.; Kosaka, T. Insight on Flavinylation and Functioning Factor in Type B Succinate Dehydrogenase from Gram-Positive Bacteria. *Biosci. Biotechnol. Biochem.* **2025**, *89* (6), 832–840. https://doi.org/10.1093/bbb/zbaf026.

(80) Cabiscol, E.; Tamarit, J.; Ros, J. Oxidative Stress in Bacteria and Protein Damage by Reactive Oxygen Species. *International Microbiology* **2000**, *3* (1), 3–8.

(81) Fasnacht, M.; Polacek, N. Oxidative Stress in Bacteria and the Central Dogma of Molecular Biology. *Front. Mol. Biosci.* **2021**, *8*, 671037. https://doi.org/10.3389/fmolb.2021.671037.

(82) Méndez, V.; Rodríguez-Castro, L.; Durán, R. E.; Padrón, G.; Seeger, M. The OxyR and SoxR Transcriptional Regulators Are Involved in a Broad Oxidative Stress Response in

Paraburkholderia Xenovorans LB400. *Biol. Res.* **2022**, *55* (1), 7. https://doi.org/10.1186/s40659-022-00373-7.

(83) Tomoyasu, T.; Tabata, A.; Imaki, H.; Tsuruno, K.; Miyazaki, A.; Sonomoto, K.; Whiley, R. A.; Nagamune, H. Role of Streptococcus Intermedius DnaK Chaperone System in Stress Tolerance and Pathogenicity. *Cell Stress Chaperones* **2012**, *17* (1), 41–55. https://doi.org/10.1007/s12192-011-0284-4.

(84) Zahn, M.; Berthold, N.; Kieslich, B.; Knappe, D.; Hoffmann, R.; Sträter, N. Structural Studies on the Forward and Reverse Binding Modes of Peptides to the Chaperone DnaK. *J. Mol. Biol.* **2013**, *425* (14), 2463–2479. https://doi.org/10.1016/j.jmb.2013.03.041.

(85) Rodríguez-Castro, L.; Méndez, V.; Durán, R. E.; Seeger, M. Long-Chain Flavodoxin FldX1 Improves Paraburkholderia Xenovorans LB400 Tolerance to Oxidative Stress Caused by Paraquat and H2O2. *PLoS One* **2019**, *14* (8), e0221881. https://doi.org/10.1371/journal.pone.0221881.

(86) Giessen, T. W.; Silver, P. A. Widespread Distribution of Encapsulin Nanocompartments Reveals Functional Diversity. *Nat. Microbiol.* **2017**, *2* (6), 17029. https://doi.org/10.1038/nmicrobiol.2017.29.

(87) Sanssouci, É.; Lerat, S.; Daigle, F.; Grondin, G.; Shareck, F.; Beaulieu, C. Deletion of TerD-Domain-Encoding Genes: Effect on Streptomyces Coelicolor Development. *Can. J. Microbiol.* **2012**, *58* (10), 1221–1229. https://doi.org/10.1139/w2012-101.

(88) Sanssouci, É.; Lerat, S.; Grondin, G.; Shareck, F.; Beaulieu, C. Tdd8: A TerD Domain-Encoding Gene Involved in Streptomyces Coelicolor Differentiation. *Antonie van*

Leeuwenhoek, International Journal of General and Molecular Microbiology **2011**, *100* (3), 385–398. https://doi.org/10.1007/s10482-011-9593-y.

(89) Langlois, P.; Bourassa, S.; Poirier, G. G.; Beaulieu, C. Identification of Streptomyces Coelicolor Proteins That Are Differentially Expressed in the Presence of Plant Material. *Appl. Environ. Microbiol.* **2003**, *69* (4), 1884–1889. https://doi.org/10.1128/AEM.69.4.1884-1889.2003.

(90) Daigle, F.; Lerat, S.; Bucca, G.; Sanssouci, édith; Smith, C. P.; Malouin, F.; Beaulieu, C. A TerD Domain-Encoding Gene (SCO2368) Is Involved in Calcium Homeostasis and Participates in Calcium Regulation of a DosR-like Regulon in Streptomyces Coelicolor. *J. Bacteriol.* **2015**, *197* (5), 913–923. https://doi.org/10.1128/JB.02278-14.

(91) Haiser, H. J.; Yousef, M. R.; Elliot, M. A. Cell Wall Hydrolases Affect Germination, Vegetative Growth, and Sporulation in Streptomyces Coelicolor. *J. Bacteriol.* **2009**, *191* (21), 6501–6512. https://doi.org/10.1128/JB.00767-09.

(92) Zhong, X.; Zhang, L.; van Wezel, G. P.; Vijgenboom, E.; Claessen, D. Role for a Lytic Polysaccharide Monooxygenase in Cell Wall Remodeling in Streptomyces Coelicolor. *mBio* **2022**, *13* (2), e00456-22. https://doi.org/10.1128/mbio.00456-22.

(93) Van Der Aart, L. T.; Spijksma, G. K.; Harms, A.; Vollmer, W.; Hankemeier, T.; Van Wezel, G. P. High-Resolution Analysis of the Peptidoglycan Composition in Streptomyces Coelicolor. *J. Bacteriol.* **2018**, *200* (20), 10–1128. https://doi.org/10.1128/JB.00290-18.

(94) Marchisio, V. F. Keratinophilic Fungi: Their Role in Nature and Degradation of Keratinic Substrates. *Rev. Iberoam. Micol.* **2000**, *17* (SUPPL.), 86–92.

(95) Ramnani, P.; Singh, R.; Gupta, R. Keratinolytic Potential of Bacillus Licheniformis RG1: Structural and Biochemical Mechanism of Feather Degradation. *Can. J. Microbiol.* **2005**, *51* (3), 191–196. https://doi.org/10.1139/w04-123.

(96) Sharma, R.; Gupta, R. Substrate Specificity Characterization of a Thermostable Keratinase from Pseudomonas Aeruginosa KS-1. *J. Ind. Microbiol. Biotechnol.* **2010**, *37* (8), 785–792. https://doi.org/10.1007/s10295-010-0723-8.

Supplementary Files

This is a list of supplementary files associated with this preprint. Click to download.

- 2SupplementaryMaterial.docx
- 3TableS1Rawdataofproteinsidentifiedineachsamplefromtheproteomicanalysis.xlsx